value of roughly 1 m is suggested if the area of rupture extended over the 3-km thickness of the crust that has been observed to host microseismicity[20], and along the 30-km length of the axis defined by the concentration of seismicity seen in Figs 1 and 3. A value of 0.5 m is suggested if rupture penetrated the full thickness of the crust.

Although the general character of the predicted 'slug-test' transient (Fig. 4) is remarkably similar to that of the observed transient (Fig. 2), the results must be considered with appropriate caution, because there are large uncertainties in applying such a simple model. For example, (1) the model considers only lateral diffusion. Ventilation through the sediment section or through faults and permeable basement outcrops (as reflected by the year-long recovery to the normal formation state, established by the thermal and hydrologic structure of the valley[13]) will 'dilute' the magnitude of the initial transient, and vertical diffusion from any extension of the dilatant volume below the transmissive uppermost crust will add to and stretch the source signal. (2) Considering the dilatation to be concentrated as a vertical line-source 'implosion' is unquestionably to oversimplify. Distributed dilatancy along the axis of the valley will create diffusional directivity (enhancing propagation across strike), and reduce the effective range between the source and the observation site along axis. (3) Perhaps the greatest shortcoming of the slug-test analogue is that it does not consider the initial distribution of elastic strain associated with the spreading event, in which quadrants of contraction (and hence volumes of positive anomalous pressure) lie next to quadrants of dilatation. Diffusion between these quadrants will produce an 'annihilation' effect near nodal planes and complicate any pressure transient generated by net dilatation. Despite these uncertainties, however, the simple concentrated-source model provides a useful first-order tool for estimating net dilatation and the hydraulic transmission properties of the formation, and for guiding a more complete analysis that will take distributed co-seismic deformation and three-dimensional diffusion into account.

We note that the co- and post-seismic pressure transients observed in ODP Hole 857D represent a significant fraction (totalling nearly 20%) of the deep-seated buoyancy that drives hydrothermal discharge at a nearby vent field. A pressure differential of +80 kPa was measured across the sediment section in ODP Hole 858G, which was drilled 1.6 km to the north into a sediment-buried permeable basement edifice beneath the vent field, sealed, and instrumented at the same time as ODP Hole 857D[12,13]. Unfortunately, the seals at this high-temperature site failed long before the earthquake swarm, but it is reasonable to conclude that basement there experienced a similar co- and post-seismic reduction in pressure. The lack of any signs of augmented hydrothermal discharge searched for during a water-column investigation of the valley carried out shortly after the swarm ended is consistent with this conclusion, as well as with our primary conclusion that the permeable crust at this site suffered net dilatancy at the time of the seismic activity. □

Methods

An outline of the relationships among strain, total stress, and pore fluid pressure in a poroelastic medium is provided in refs 11 and 21. The elastic properties involved are either established by laboratory data (at conditions corresponding to the formation temperature and pressure of 280 °C and 30 MPa, respectively), by observations of cored material, or by observed formation-fluid pressure response to tidal loading. These include: fluid compressibility, $\beta_f = 1.3 \times 10^{-9}\,\mathrm{Pa}^{-1}$; solid constituent compressibility, $\beta_s = 2.0 \times 10^{-11}\,\mathrm{Pa}^{-1}$; one-dimensional tidal loading efficiency, $\gamma = 0.14$; matrix frame compressibility, $\beta_m = 6.8 \times 10^{-11}\,\mathrm{Pa}^{-1}$; porosity, $n = 0.15$; and Poisson's ratio, $\nu = 0.25$. The resulting linear coefficient relating strain and fluid pressure is $0.29 \times 10^{-9}\,\mathrm{Pa}^{-1}$. The relationship between permeability k and hydraulic diffusivity η involves a subset of these properties plus viscosity $\mu = 10^{-4}$ Pa s (appropriate for the formation temperature): $k = \mu\xi\eta$, where ξ, the storage compressibility, is a function of n, β_f, β_s and β_m as outlined in ref. 21.

Received 15 January; accepted 14 June 2004; doi:10.1038/nature02755.

1. Baker, E. T. *et al.* Hydrothermal event plumes from the CoAxial seafloor eruption site, Juan de Fuca Ridge. *Geophys. Res. Lett.* **22,** 151–154 (1995).
2. Embley, R. W., Chadwick, W. W., Jonasson, I. R., Butterfield, D. A. & Baker, E. T. Initial results of the rapid response to the 1993 CoAxial event: Relationships between hydrothermal and volcanic processes. *Geophys. Res. Lett.* **22,** 143–146 (1995).
3. Von Damm, K. L. *et al.* Evolution of East Pacific Rise hydrothermal vent fluids following a volcanic eruption. *Nature* **395,** 47–50 (1995).
4. Dziak, R. P., Fox, C. G. & Schreiner, A. E. The June-July 1993 seismoacoustic event at CoAxial Segment, Juan de Fuca Ridge: Evidence for a lateral dike injection. *Geophys. Res. Lett.* **22,** 135–138 (1995).
5. Sohn, R. A., Fornari, D. J., Von Damm, K. L., Hildebrand, J. A. & Webb, S. C. Seismic and hydrothermal evidence of a cracking event on the East Pacific Rise crest near 9° 50′ N. *Nature* **396,** 159–161 (1998).
6. Delaney, J. R. *et al.* The quantum event of ocean crustal accretion: Impacts of diking at mid-ocean ridges. *Science* **281,** 222–230 (1998).
7. Dziak, R. P. & Fox, C. G. The January 1998 earthquake swarm at Axial Volcano, Juan de Fuca Ridge: Hydroacoustic evidence of seafloor volcanic activity. *Geophys. Res. Lett.* **26,** 3429–3432 (1999).
8. Lupton, J. E., Baker, E. T. & Massoth, G. J. Helium, heat, and the generation of hydrothermal event plumes at mid-ocean ridges. *Earth Planet. Sci. Lett.* **171,** 343–350 (1999).
9. Johnson, H. P. *et al.* Earthquake-induced changes in a hydrothermal system at the Endeavour Segment, Juan de Fuca Ridge. *Nature* **407,** 174–177 (2000).
10. Lilley, M. D., Butterfield, D. A., Lupton, J. E. & Olson, E. J. Magmatic events can produce rapid changes in hydrothermal vent chemistry. *Nature* **422,** 878–881 (2003).
11. Davis, E. E., Wang, K., Thomson, R. E., Becker, K. & Cassidy, J. F. An episode of seafloor spreading and associated plate deformation inferred from crustal fluid pressure transients. *J. Geophys. Res.* **106,** 21953–21963 (2001).
12. Davis, E. E., Becker, K., Pettigrew, T., Carson, B. & Macdonald, R. CORK: A hydrologic seal and downhole observatory for deep-ocean boreholes. *Proc. ODP Init. Rep.* **139,** 43–53 (1992).
13. Davis, E. E. & Becker, K. Formation temperatures and pressures in a sedimented rift hydrothermal system: Ten months of CORK observations, Holes 857D and 858G. *Proc. ODP Sci. Res.* **139,** 649–666 (1994).
14. Jonsson, S., Segall, P., Pedersen, R. & Bjornsson, G. Post-earthquake ground movements correlated to pore-pressure transients. *Nature* **424,** 179–183 (2003).
15. Okada, Y. Internal deformation due to shear and tensile faults in a half space. *Bull. Seismol. Soc. Am.* **82,** 1018–1040 (1992).
16. Cooper, H. H. Jr, Bredehoeft, J. D. & Papadopulos, I. S. Response of a finite diameter well to an instantaneous charge of water. *Wat. Resour. Res.* **3,** 263–269 (1967).
17. Becker, K., Morin, R. H. & Davis, E. E. Permeabilities in the Middle Valley hydrothermal system measured with packer and flowmeter experiments. *Proc. ODP. Sci. Res.* **139,** 613–626 (1994).
18. Bessler, J. U., Smith, L. & Davis, E. E. Hydrologic and thermal conditions at a sediment/basalt interface: Implications for interpretation of field measurements at Middle Valley. *Proc. ODP Sci. Res.* **139,** 667–678 (1994).
19. Davis, E. E. & Villinger, H. Tectonic and thermal structure of the Middle Valley sedimented rift, northern Juan de Fuca Ridge. *Proc. ODP Init. Rep.* **139,** 9–41 (1992).
20. Golden, C. E., Webb, S. C. & Sohn, R. A. Hydrothermal microearthquake swarms beneath active vents at Middle Valley, northern Juan de Fuca Ridge. *J. Geophys. Res.* **108,** doi:10.1029/2001JB000226 (2003).
21. Wang, K. Applying fundamental principles and mathematical models to understand processes and estimate parameters. In *Hydrogeology of the Oceanic Lithosphere* (eds Davis, E. E. & Elderfield, H.) (Cambridge Univ. Press, in the press).
22. Fox, C. G., Dziak, R. P., Marumoto, H. & Schreiner, A. E. Potential for monitoring low-level seismicity on the Juan de Fuca Ridge using military hydrophone arrays. *Mar. Technol. Soc. J.* **27,** 22–30 (1994).

Acknowledgements We acknowledge the Ocean Drilling Program for ongoing support for long-term borehole monitoring experiments, T. Pettigrew, R. Meldrum, and R. Macdonald for engineering assistance, R. Thomson and S. Mihaley for assistance with the post-swarm water-column survey on board CHS Tully, M. Fowler for assistance with SoSUS data processing, and J. Risteau for earthquake moment tensor calculations. Financial support was provided by the US National Science Foundation and by the Geological Survey of Canada.

Competing interests statement The authors declare that they have no competing financial interests.

Correspondence and requests for materials should be addressed to E.E.D. (edavis@nrcan.gc.ca).

Cladogenesis and morphological diversification in passerine birds

Robert E. Ricklefs

Department of Biology, University of Missouri-St Louis, 8001 Natural Bridge Road, St Louis, Missouri 63121-4499, USA

Morphological diversity tends to increase within evolving lineages over time[1,2], but the relative roles of gradual evolutionary change (anagenesis)[3] and abrupt shifts associated with speciation events (cladogenesis, or 'punctuated equilibrium')[4] have not been resolved for most groups of organisms[5]. However,

these two modes of evolution can be distinguished by the fact that morphological variance increases in proportion to time under anagenesis[6], and in proportion to the logarithm of the number of species under cladogenesis[7]. Although species and time are themselves correlated, multiple regression analysis provides a statistical framework for partitioning their relative contributions. In this study, I use multiple regressions to evaluate the effects of time and species number on morphological diversity within clades of passerine birds. The results show clearly that number of species exerts a strong influence on morphological variance independent of time, but that time has no unique effect. Thus, morphological evolution in birds seems to be associated with cladogenesis. How lineage splitting promotes morphological diversification poses an important challenge to ecologists and evolutionary biologists.

I quantified morphological variation by the variance of principal component (PC) scores within tribe-to-family-level clades of passerine birds (Supplementary Table 1) based on eight log-transformed external measurements (for example, wing, leg and beak; see Methods). These variables characterize structure related to diet, substrate use and habitat[8,9]. The variances provide convenient indices to diversity because the PC axes have dimensionless scales, distances between species in morphological space are conserved and the estimate of the variance is independent of both sample size and the average value of the measurement variables[1,10].

I evaluated the contributions of taxon age (see Methods) and species richness to morphological variation by multiple regression. Using this approach, the unique statistical effects of age and species richness can be estimated, independently of any correlation between the two. Morphological variance within the entire sample of clades ($n = 95$) was unrelated to variation in the relative age of clades ($P > 0.18$ for all PC axes), but increased significantly ($P < 0.05$) with respect to the logarithm of species on all principal components, except PC4, PC5 and PC8 (Fig. 1a). When age was dropped from the analysis and continental versus non-continental distribution was included as an effect, morphological variances on PC4 ($P = 0.0003$) and PC8 ($P = 0.006$) were also significantly related to species number (Fig. 1b).

In many clades of birds distributed in southeast Asia, including Indonesia, the Philippines and Australasia, numerous differentiated island populations have been given species names. To avoid potentially uninformative variation introduced by these clades, I performed a second analysis restricted to continental clades, with undersampled taxa also removed (see Methods). Among these 50 clades, relative age remained insignificant in both simple and multiple regressions. When age was removed as a variable, the relationship of morphological variance to logarithm of the number of species was significant for all principal components ($P < 0.0001$; $P = 0.0049$ (PC5) and $P = 0.0008$ (PC8)), except PC7 ($P = 0.19$). Number of species alone explained 15.3% to 43.6% of the variation among clades on individual PC axes, and 33.3% of the total variation. These results were independent of the proportion of species sampled per clade (all $P > 0.05$).

Because the relative ages of clades varied by only a factor of four (see Methods), these analyses might not have included a sufficient range to detect an effect of time on morphological variance. Indeed, age and the log-transformed number of species per clade were unrelated in the entire sample of clades ($r = -0.135$, $P = 0.19$, $n = 95$), and morphological variance was unrelated to age alone in simple correlations (all $P > 0.12$). To provide a broader range of clade age, I calculated morphological variances within 108 genera (having five or more species sampled) and included these in a multiple regression with tribe-to-family-level clades. In the analysis, morphological variance was significantly related to age alone on all PC axes ($P < 0.01$); this was as expected because the logarithm of species number was also significantly correlated with relative age ($r = 0.55$, $P < 0.0001$). However, the effect of age in multiple regressions was insignificant for all axes ($P > 0.05$) except PC5 ($P = 0.016$). As found before, the effect of the logarithm of species number was significant ($P < 0.006$ for all PC axes, and <0.0001 for PC1, 2, 3 and 5), accounting for 9.1% to 24.1% of the morphological variance. Thus, morphological variance does not increase over time independently of species production, and I conclude that the proliferation of species is the primary driver of morphological diversification within clades of passerine birds.

In spite of the significant relationship between morphological diversity and species richness, considerable variation remains. Factors besides species formation *per se* that could influence morphological diversity include: (1) the complexity of the environment as a template for morphological adaptation[11–13]; (2) the constraining influence of other species, particularly potential competitors, within the distribution of a diversifying clade; and (3) diversifying selection from competition by secondarily sympatric sister taxa[11,14–17].

The environmental template undoubtedly is clade-specific and difficult to evaluate. Although large and small clades coexist regionally, whether the availability of ecological space limits diversification cannot be easily addressed. One might expect islands to present more limited ecological opportunities than continental

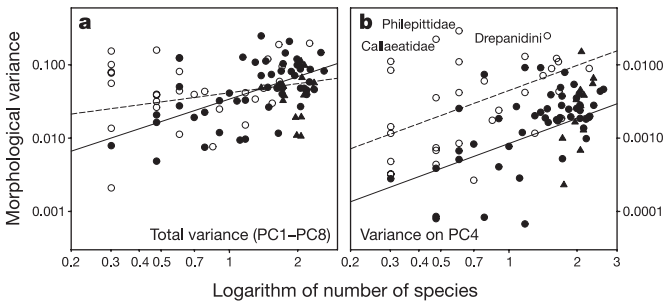

Figure 1 The relationship between morphological variance and number of species for 95 passerine clades. Clades distributed in non-continental (open symbols) and continental (solid symbols) regions, and undersampled clades (triangles). **a**, Total variance (PC1–PC8). Dashed regression line includes all 95 clades (slope = 0.415 ± 0.141 s.e.m.); solid regression line includes only well-sampled continental clades ($n = 50$, slope = 1.016 ± 0.208 s.e.m.). **b**, PC4 (relative beak length). Dashed regression line for non-continental clades (elevation = 0.723 ± 0.180 s.e.m.); solid regression line for all continental clades (common slope = 1.134 ± 0.306 s.e.m.).

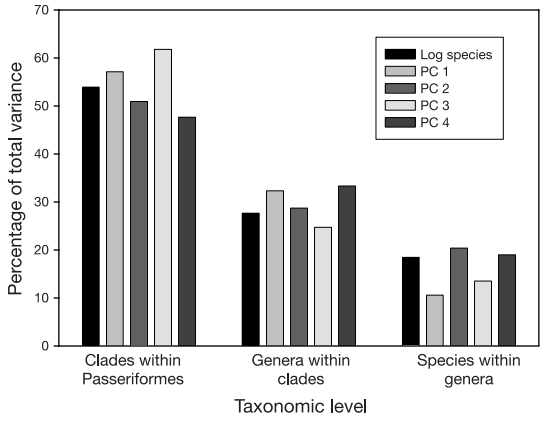

Figure 2 Distribution of morphological variance on PC axes 1–4. Values estimated by hierarchical nested analysis of variance compared to the value expected if morphology diversified in direct relation to the logarithm of the average number of species within evolutionary lineages (black bars).

landmasses; however, even most non-continental clades have diversified within large, ecologically complex regions. As explained below, non-continental clades of comparable size have no less morphological variance than those that have diversified within continental landmasses.

To evaluate the constraining influence of regional diversity, I compared morphological variance between clades in continental and non-continental areas. Many non-continental tribe-to-family-level lineages of passerine birds occur on islands or island-continents (including New Guinea, New Zealand, Madagascar and Australia) where morphological space presumably has been less densely occupied than in the major continental landmasses of Africa, Eurasia, and North and South America. Variance within continental clades was less than that in island clades on all morphological axes (binomial $P = 0.004$). However, the only axis showing a significant continent/non-continent effect in the overall analysis ($n = 95$) was PC4, which is correlated with the length of the beak relative to the size of the foot. Variance on this axis in non-continental clades exceeded that in continental clades ($F_{1,92} = 16.1$, $P < 0.0001$) by 0.72 ± 0.18 (mean $\pm$ s.e.m.) $\log_{10}$ units, or a factor of 5.2 (Fig. 1b). This axis is associated with variation in diet, feeding method and substrate use in birds, and it probably represents an axis along which birds can easily diverge ecologically.

A range of beak morphology, from greatly elongated to massively stout, characterizes many island passerine clades. Three of these with extreme variation on PC4 are indicated in Fig. 1b: the New Zealand wattlebirds (Callaeatidae), the Malagasy asities (Philepittidae) and the Hawaiian honeycreepers (Drepanidini). These unusual radiations of non-continental forms might reflect open ecological space on islands allowing novel avenues of morphological change. Indeed, the beak morphology of the Hawaiian honeycreepers fills most of the morphological space occupied by passerine birds[18].

To test the effect of diversifying selection, I further related morphological variation to the extent of sympatry (see Methods) among species within small clades. Diversifying selection should be most intense when sister lineages gain secondary sympatry and compete strongly for shared resources[15,17,19]. The potential effect of both factors was explored for clades with fewer than ten species ($n = 32$), that exhibited the full range of morphological variance (see Fig. 1) and could be scored easily for degree of sympatry (see Supplementary Table 2), and also could be designated as either continental or non-continental.

Morphological variances were higher among non-continental clades on all axes except PC7 (binomial $P = 0.035$), but the effects were not significant by themselves on any of the PC axes. Variance increased with respect to the sympatry index on all eight PC axes ($P = 0.004$), but significantly only on PC4 ($P = 0.014$). Thus, among small clades, morphological diversification tends to be accelerated on islands and by selection following secondary sympatry, but neither effect is strong.

Whatever the cause of diversification, if morphological change associated with speciation events were random and homogeneous, the relationship between morphological variance and the logarithm of species number would be linear. Accordingly, the slope of the regression between the logarithm of the variance and the double logarithm of species number would be 1.0. Higher slopes would indicate acceleration of morphological diversification with species number; lower slopes would indicate constrained diversification with increasing species richness. Among the well-sampled continental clades ($n = 50$), the slope (b) of this relationship exceeded one for PC1 ($b = 1.74 \pm 0.34$ s.e.m., $t = 2.18$, $P = 0.034$) and PC3 ($b = 1.54 \pm 0.26$ s.e.m., $t = 2.22$, $P = 0.034$). The total variance in the smaller PC axes increased at a lower rate than the logarithm of species number (PC5–8 combined, $b = 0.49 \pm 0.15$ s.e.m., $t = -3.40$, $P = 0.0029$). Thus, some components of morphological variance increase disproportionately more rapidly than the number of species per clade, but these are balanced by some that increase more slowly. The resulting total morphological variance (PC1–8) increased as the 1.02 ± 0.21 s.e.m. power of the logarithm of species number.

This direct proportionality of morphological diversification with the logarithm of the number of species extends to the entire sample of passerine birds. Total morphological variance among all passerines (clade size = 5,712 species) was 111% of the extrapolated values for the sum of PC1–8 (based on the regression of variance on species number among well-sampled continental clades). Thus, diversification does not seem to be constrained by existing diversity.

The distribution of morphological variance among taxonomic levels provides an additional indication that diversification is unconstrained by increasing species number. If variance increased uniformly with the logarithm of species number, it would be distributed as 53.9% among 106 tribe-to-family-level clades within Passeriformes, 27.7% among an average of 10.95 genera within clades and 18.4% among an average of 4.9 species within genera. Morphological variance corresponds closely to this expectation, as shown for the first four PC axes in Fig. 2. The hierarchical distribution of variance argues that recent lineage splitting, represented by the species-within-genus component of variance, has resulted in continued morphological diversification along all axes of variation.

The filling of morphological space probably has not constrained speciation either. Tribe-to-family-level clades show no evidence of regulation of species richness in terms of the expected variation in number of species among clades[20]. That is, large tribe-to-family-level clades are not fewer than predicted by the geometric distribution produced by a random speciation-extinction model. Diversification of passerine birds with respect to both species richness and morphology seems to be unrestrained globally. Whether or not increasing species number results in finer local partitioning of geography or habitat that is unrelated to morphology, larger clades also generate greater morphological diversity.

Morphological diversification in passerine birds is strongly associated with species rather than time *per se*. However, the strong species effect on morphological diversity identified in this analysis does not necessarily imply punctuated equilibrium—change associated with the speciation process itself[4,21]. Speciation can also promote evolutionary diversification indirectly by establishing selection for divergent evolution in evolutionarily independent lineages. Thus, divergent evolution might occur gradually over long periods following lineage splitting rather than as an abrupt consequence of the formation of new species in small, peripherally isolated populations forced to undergo rapid reorganization of their gene pools[22]. Although secondary sympatry of sister species is likely to create strong selection for divergence[15,16,19], newly formed lineages in species-rich clades might also face sufficient selective pressure from more distantly related species, to diversify morphologically in allopatry. Mechanisms linking morphological diversity to species richness can be investigated more readily by relating divergence to age, distribution and ecology in studies focused on individual clades. □

Methods

Taxonomy

This analysis is limited to passerine birds (the monophyletic order Passeriformes, 5,712 species), which include more than half of all bird species. I use the 106 smallest non-nested suprageneric taxa designated as monophyletic groups (tribes, subfamilies or families) in the treatment of Sibley and Monroe[23] (see Supplementary Table 1). Age was estimated as the depth of the node uniting each group with its sister taxon, obtained by DNA hybridization and expressed as the difference in temperature at 50% dissociation (the melting point temperature, $\Delta T_{50}H$) between heteroduplexed and homoduplexed DNA (°C)[24]. Relative ages of the 106 taxa ranged between 4.3 and 17.9 °C and number of species varied between 1 and 413. Number of species was independent of deeper phylogenetic relationships among clades[24] according to Abouheif's test[25] of serial phylogenetic independence ($n = 106$, $P = 0.155$).

Measurements and samples

The following measurements were obtained with calipers and rulers from museum skins: total length, wing and tail (in mm); tarsus, middle toe, and the length, width and breadth

of the culmen (0.1 mm)[10]. Measurements were averaged within species. Altogether, the data set comprised 1,018 (17.8% of 5,712) species in 103 (97.2% of 106) suprageneric taxa of passerine birds.

Two samples of tribe-to-family-level clades were analysed. The most inclusive contained the 95 taxa for which I measured more than one species and could therefore calculate morphological variance. The second sample ($n = 50$) excluded clades restricted to non-continental landmasses (primarily Australasia, New Zealand, Madagascar and the Greater Antilles), as well as tribe-to-family-level clades for which I measured fewer species than one-third the number of genera or one-tenth the number of species.

In a further analysis, I extended the range of clade age by including estimates of morphological variance within 108 genera having five or more species and for which I had measured more than 20% of all species. Genera were assigned a relative age of $\Delta T_{50}H = 3.2$ °C (the median relative age of nodes within subtribes)[24]. These were combined with well-sampled tribe-to-family-level clades.

Sympatry within small clades

I used distribution maps in field guides and handbooks to estimate by eye the approximate degree of sympatry among the species in clades having fewer than ten species (see Supplementary Table 2). For each clade, the sympatry index is the proportion of species (0–1) having greater than ≈50% overlap in their geographic range with one or more other species in the clade, hence having the potential for interacting locally.

Analyses

The eight morphological values were $\log_{10}$-transformed to make the distribution of variation in each of the measurements dimensionless, approximately normal within the sample of species and unrelated to the mean value of the measurement. Over all species, standard deviations of the log-transformed measurements varied between 0.144 and 0.195 (equivalent to factors of 1.39 and 1.57) and thus large and small measurements contributed comparably to distance between species in morphological space. Log-transformed measurements were subjected to a principal components (PC) analysis based on the covariance matrix, to reduce the dimensionality of the data and obtain uncorrelated axes of morphological variation. Using the covariance matrix preserves the original euclidean distances between species[26].

The first PC axis incorporated 75% of the variance in morphology and the first three axes incorporated 91%. The resulting eight PC scores for each species were then used to estimate the variance on each of the PC axes for each tribe-to-family-level clade. The estimate of the variance is unbiased with respect to sample size[1]. Among 95 clades, the morphological standard deviation was phylogenetically independent according to Abouheif's test[25] for PC1 ($P = 0.55$) and PC4 ($P = 0.17$).

To test the hypothesis that morphological diversification is a function of number of species, time or both, I used multiple regression to determine the relationship between morphological variance on each of the PC axes and the logarithm of species number and relative age of each clade. Each of the variables was log-transformed to make the deviations of morphological variance about the regression uniform and to test the linearity of the relationship (slope = 1).

I conducted nested analyses of variance to examine the distribution of variation among species within genera, genera within tribe-to-family-level clades, and clades within passerines. The expected morphological variation depending on a direct relationship to the logarithm of species was calculated as follows: the logarithm of the number of smaller taxa within each larger taxon at each level in the hierarchy of analysis (that is, 106 clades within passerines, 10.95 genera per clade and 4.92 species per genus).

All analyses were performed using the Statistical Analysis System (SAS Institute, Cary, North Carolina).

Received 3 November 2003; accepted 24 May 2004; doi:10.1038/nature02700.

1. Foote, M. The evolution of morphological diversity. *Annu. Rev. Ecol. Syst.* **28,** 129–152 (1997).
2. Harmon, L. J., Schulte, J. A. II, Larson, A. & Losos, J. B. Tempo and mode of evolutionary radiation in iguanian lizards. *Science* **301,** 961–964 (2003).
3. Simpson, G. G. *The Major Features of Evolution* (Columbia Univ. Press, New York, 1953).
4. Gould, S. J. & Eldredge, N. Punctuated equilibria: the tempo and mode of evolution reconsidered. *Paleobiology* **3,** 115–151 (1977).
5. Jackson, J. B. C. & Cheetham, A. H. Tempo and mode of speciation in the sea. *Trends Ecol. Evol.* **14,** 72–77 (1999).
6. Raup, D. M. & Gould, S. J. Stochastic simulation and evolution of morphology–towards a nomothetic paleontology. *Syst. Zool.* **23,** 305–322 (1974).
7. Foote, M. in *Evolutionary Paleobiology* (eds Jablonski, D., Erwin, D. H. & Lipps, J. H.) 62–86 (Univ. Chicago Press, Chicago, 1996).
8. Miles, D. B. & Ricklefs, R. E. The correlation between ecology and morphology in deciduous forest passerine birds. *Ecology* **65,** 1629–1640 (1984).
9. Ricklefs, R. E. & Miles, D. B. in *Ecological Morphology. Integrative Organismal Biology* (eds Wainwright, P. C. & Reilly, S. M.) 13–41 (Univ. Chicago Press, Chicago, 1994).
10. Ricklefs, R. E. & Travis, J. A morphological approach to the study of avian community organization. *Auk* **97,** 321–338 (1980).
11. Benkman, C. W. Divergent selection drives the adaptive radiation of crossbills. *Evolution* **57,** 1176–1181 (2003).
12. Moritz, C., Patton, J. L., Schneider, C. J. & Smith, T. B. Diversification of rainforest faunas: an integrated molecular approach. *Annu. Rev. Ecol. Syst.* **31,** 533–563 (2000).
13. Schluter, D. Morphological and phylogenetic relations among the Darwin's finches. *Evolution* **38,** 921–930 (1984).
14. Lack, D. *Darwin's Finches* (Cambridge Univ. Press, Cambridge, 1947).
15. Grant, P. R. Convergent and divergent character displacement. *Biol. J. Linn. Soc.* **4,** 39–68 (1972).
16. Schluter, D. Character displacement and the adaptive divergence of finches on islands and continents. *Am. Nat.* **131,** 799–824 (1988).
17. Schluter, D. Ecological causes of adaptive radiation. *Am. Nat.* **148,** S40–S64 (1996).
18. Lovette, I. J., Bermingham, E. & Ricklefs, R. E. Clade-specific morphological diversification and adaptive radiation in Hawaiian songbirds. *Proc. R. Soc. Lond. B* **269,** 37–42 (2002).
19. Schluter, D. *The Ecology of Adaptive Radiation* (Oxford Univ. Press, Oxford, 2000).
20. Ricklefs, R. E. Global diversification rates of passerine birds. *Proc. R. Soc. Lond. B* **270,** 2285–2291 (2003).
21. Eldredge, N. & Gould, S. J. in *Models in Paleobiology* (ed. Schopf, T. J. M.) 82–115 (Freeman, San Francisco, 1972).
22. Carson, H. L. & Templeton, A. R. Genetic revolutions in relation to speciation phenomena: the founding of new populations. *Annu. Rev. Ecol. Syst.* **15,** 97–131 (1984).
23. Sibley, C. G. & Monroe, B. L. Jr. *Distribution and Taxonomy of Birds of the World* (Yale Univ. Press, New Haven, Connecticut, 1990).
24. Sibley, C. G. & Ahlquist, J. E. *Phylogeny and Classification of the Birds of the World* (Yale Univ. Press, New Haven, Connecticut, 1990).
25. Abouheif, E. A method to test the assumption of phylogenetic independence in comparative data. *Evol. Ecol. Res.* **1,** 895–909 (1999).
26. Legendre, P. & Legendre, L. *Numerical Ecology* (Elsevier, Amsterdam, 1998).

Supplementary Information accompanies the paper on **www.nature.com/nature**.

Acknowledgements I thank M. Foote, T. Givnish and S. S. Renner for constructive comments. For access to specimens, I am grateful to curators and collection managers at the Academy of Natural Sciences in Philadelphia, the US National museum, the American Museum of Natural History, the Field Museum in Chicago, the Bavarian State Collections in Munich, the Senckenberg Museum in Frankfurt and the Museum des Sciences Naturelles in Brussels. This work was supported in part by research funds available to Curators' Professors at the University of Missouri.

Competing interests statement The authors declare that they have no competing financial interests.

Correspondence and requests for materials should be addressed to R.E.R. (ricklefs@umsl.edu).

The combined effects of pathogens and predators on insect outbreaks

Greg Dwyer[1], Jonathan Dushoff[2] & Susan Harrell Yee[1]

[1]*Department of Ecology and Evolution, 1101 E 57th Street, University of Chicago, Chicago, Illinois 60637-1573, USA*
[2]*Department of Ecology and Evolutionary Biology, Princeton University, Princeton, New Jersey 08544, USA*

The economic damage caused by episodic outbreaks of forest-defoliating insects has spurred much research[1], yet why such outbreaks occur remains unclear[2]. Theoretical biologists argue that outbreaks are driven by specialist pathogens or parasitoids, because host–pathogen and host–parasitoid models show large-amplitude, long-period cycles resembling time series of outbreaks[3,4]. Field biologists counter that outbreaks occur when generalist predators fail, because predation in low-density defoliator populations is usually high enough to prevent outbreaks[5–8]. Neither explanation is sufficient, however, because the time between outbreaks in the data is far more variable than in host–pathogen and host–parasitoid models[1,2], and far shorter than in generalist-predator models[9–11]. Here we show that insect outbreaks can be explained by a model that includes both a generalist predator and a specialist pathogen. In this host–pathogen–predator model, stochasticity causes defoliator densities to fluctuate erratically between an equilibrium maintained by the predator, and cycles driven by the pathogen[12,13]. Outbreaks in this model occur at long but irregular intervals, matching the data. Our results suggest that explanations of insect outbreaks must go beyond classical models to consider interactions among multiple species.

The host–pathogen model that we begin with describes the effects of a specialist pathogen on the population dynamics of a forest defoliator. Host-specific pathogens of defoliators are often baculoviruses, which cause fatal diseases transmitted when larvae